Friction Estimation by Pressing an Elastic Finger-Shaped Sensor Against a Surface

Takashi Maeno, *Member, IEEE*, Tomoyuki Kawamura, and Sen-Chieh Cheng

***Abstract*—A method is proposed to estimate the friction coefficient between a planar surface and an elastic finger-shaped sensor by only pressing a sensor against the surface of an object. The contact condition between a planar surface and a half-cylindrical finger is considered, using finite-element analysis. The deformation of the elastic finger, contact forces, and strain distribution inside the elastic finger are calculated for various friction coefficients between the finger and the surface. Results show that the shear strain differs when the friction coefficient differs. In addition, in this paper, an elastic finger-shaped sensor made of silicone rubber is designed and constructed. In an experiment using this newly designed sensor, the friction coefficient between the finger and the planar surface is estimated using the strain inside the finger.**

***Index Terms*—Contact problem, friction, friction coefficient, grasp, robot finger, sensors, tactile sensors.**

I. Introduction

In the field of robotics, one of the most important problems is the development of robot hands that can grip and lift objects avoiding slippage and crushing, even when the weight and friction coefficients are unknown. A variety of techniques for lifting objects have been proposed, and these can be classified into the following three methods. The first method involves detecting the microvibration of a finger when the object starts slipping [1]–[4]. However, this method produces slippage, and is not adequate for precise positioning because the object moves slightly in the lifting direction.

The second method involves detecting partial incipient slippage between a finger and an object. The partial slippage refers to the contact condition between two bodies in which a part of the contact area "slips" and the other part "sticks" or "adheres." Tremblay *et al.* [5] proposed a method to detect the localized slip between a sensor and an object that precedes gross slip. They detected the vibration due to the localized slip using two acceleration sensors, and estimated the friction coefficient using the ratio of the tangential and normal force. Using this method, they could clearly detect the incipient slippage. However, the value of the estimated friction coefficient was not accurate. Canepa [6] and Maeno [7] detected the partial incipient slippage of the object using a skin-like sensor. They used the distribution pattern of the stress/strain inside the elastic finger to detect the partial slip information. This is similar to what human beings do [8]. However, this method requires a large number of sensors incorporated in an elastic body, as well as a pattern-recognition technique.

The third method involves estimation or direct measurement of the friction coefficient between the finger and an object. Bicchi [9], [10] estimated the friction coefficient between a force-torque tactile sensor and the object. However, the estimated value of the friction coefficient was obtained after the entire slippage occurs. Yamada [11] presented a method to directly measure a friction coefficient by rotating a disk placed in a robot hand. This method is useful when avoiding slippage, since the normal and tangential forces can easily be controlled by using the friction cone between two objects calculated from the measured friction coefficient. However, the equipment becomes large and heavy.

Detecting a friction coefficient is important for robot hands to grip and lift objects while avoiding slippage and crushing. By detecting the friction coefficient and controlling the normal force so that the tangential force is within the friction cone, it is easily possible for the robot hand to manipulate objects without slipping. However, because of the problems mentioned above, a method is required to obtain the friction coefficient without entire slippage and by using a simple sensor. Detecting the friction coefficient between the robot hand and object is also necessary in cases such as complex handling of the object, input/output devices for virtual reality on a haptic interface, and robots to handle objects in factory automation.

On the other hand, human beings can grip and lift various objects, even when the weight and the friction coefficient are unknown. How are we able to do this? Johansson [8] measured the nerve signals and normal/tangential forces simultaneously when human fingers gripped and lifted several kinds of objects having planar surface. It was shown that the frequency of nerve signals just after the finger has touched the object differs from when the friction coefficient between the finger and object differs. When the friction coefficient is small, i.e., in the case of silk, frequency of the nerve signal is large. Conversely, when the friction coefficient is large, i.e., in the case of sandpaper, frequency of the nerve signal is small. We can conclude that the difference of the frictional coefficient is already distinguished slightly after the time the fingers are in contact with the object. From this, we hypothesize that the friction coefficient between an artificial finger and object can be estimated by indenting the object into an artificial finger-shaped elastic sensor. A similar

Manuscript received September 24, 2002; revised April 7, 2003. This paper was recommended for publication by Associate Editor P. Dupont and Editor A. De Luca upon evaluation of the reviewers' comments.

T. Maeno is with the Department of Mechanical Engineering, Keio University, Hiyoshi, Yokohama 223-8522, Japan (e-mail: maeno@mech.keio.ac.jp).

T. Kawamura was with Keio University, Hiyoshi, Yokohama 223-8522, Japan. He is now with Hitachi Ltd., Totsuka, Yokohama 244-0817, Japan (e-mail: PXP07317@nifty.ne.jp).

S.-C. Cheng was with Keio University, Hiyoshi, Yokohama 223-8522, Japan. He is now with Shinkawa Ltd., Tokyo 208-8585, Japan (e-mail: dynasty@mx9.ttcn.ne.jp).

Digital Object Identifier 10.1109/TRA.2003.820850

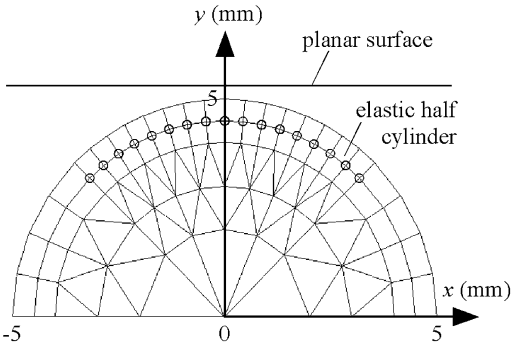

Fig. 1. FE model of a simple half-cylindrical finger cross-section.

idea was also introduced by Shinoda [12]. They showed that the tangential stress/strain at the center of the finger indicates the change in friction coefficient.

In this paper, we solve the contact problem between a half-cylindrical finger and a planar surface with different friction coefficients, when the surface is indented into the finger. We show that the shear strain, rather than tangential strain at the center, most clearly indicates the change in frictional coefficient between the two bodies. In addition, in this paper, an elastic finger-shaped sensor made of silicone rubber is designed and constructed. The sensor has strain gauges incorporated near the edge of the contact region, and the locations and angles of the strain gauges are determined such that the strain varies when the friction coefficient varies. Finally, an experiment is performed in order to verify the proposed method.

II. Finite Element (FE) Analysis to Verify the Method

A. Model and Method for Contact Analysis

Contact between an elastic finger with a curved surface and an object with a planar surface is analyzed using the finite-element method (FEM). Fundamental contact conditions between the elastic finger and the planar surface are analyzed by assuming the Coulomb friction, taking into account partial incipient slip. The purpose of this analysis is to show that frictional information regarding the part of the surface in contact with the elastic finger can be indicated by the shear strain inside the elastic finger.

A finger-shaped sensor is modeled as a simple half-cylindrical finger with a radius of 5 mm, as shown in Fig. 1. The shape of the finger does not have to be half-cylindrical, but it must have a curved surface. By using a curved surface instead of a flat one, the normal reaction force is distributed, and the stick and slip regions appear at specific regions at the edge of the contact area, as described later in Section II-B.

Normal load is changed by increasing forced displacements of the planar surface 0.1 mm in the y direction per interval, until the displacement reaches 1 mm. The nodes at $y = 0$ are constrained in the x and y directions. The FE model consists of 96 nodes and 108 elements. The elastic modulus of the finger is 1 MPa. Plane stress elements are used, and nonlinearity due to large deformation is neglected. Friction coefficients are changed from 0.06 to 1.0.

There are many commercialized FE codes that are capable of solving the contact between two elastic bodies. However, normal/tangential reaction force and stick/slip conditions at the contact interface cannot usually be calculated accurately using these codes, since their convergence is calculated based solely on displacement error. Even if the displacement error is small, error of the derivatives of the displacement are usually larger. It affects the stick/slip condition significantly, because the stick/slip phenomena depend on the derivatives of the displacement. Therefore, to analyze the time-dependent contact problem, we proposed a method that can obtain the stick/slip condition in the tangential direction accurately, and so avoid these errors [7]. Discrete time and space are defined in a simulation, because the method is based on iterative FE analysis.

Nodes at the surface of the elastic finger should satisfy the following equations:

$$\text{noncontact nodes} : w_n < w_{\text{object}}, \quad f_n = 0 \tag{1}$$

$$\text{contact nodes} : w_n = w_{\text{object}}, \quad f_n > 0 \tag{2}$$

$$\text{sticking nodes} : w_t = w_t', \quad |f_t| < \mu |f_n| \tag{3}$$

$$\text{slipping nodes} : |f_t| = \mu |f_n| \tag{4}$$

where w_n and w_t are the locations in the normal and tangential directions, f_n and f_t are the nodal forces in the normal and tangential directions, respectively, w_{object} is the normal location of the object, and μ is the friction coefficient. Although the static friction coefficient is usually larger than the kinetic friction coefficient, these values are assumed the same in the fundamental calculation to simplify the argument. The prime represents values in the previous time frame.

The contact problem for a specific time is solved by the following procedure. First, the nodes in contact with the object in the previous time frame are assumed to satisfy (2) and (3) in the present time, i.e., the nodes are constrained to remain stuck and in contact. The surface nodes not in contact with the object in the previous time frame are assumed to satisfy (1), i.e., the nodes are not constrained. Then an FE analysis is performed. The result of the FE analysis is evaluated if (1)-(4) are satisfied at all nodes at the surface. Nodes that do not satisfy (1) are assumed to be contact nodes that satisfy (2). Conversely, nodes that do not satisfy (2) are assumed to be noncontact nodes that satisfy (1). Nodes that do not satisfy (3) are changed to be slipping nodes that satisfy (4), i.e., the friction force is applied. The calculation is repeated as contact conditions are changed until (1)-(4) are completely satisfied at all the nodes at the surface. When these conditions have been satisfied, we move to the next time frame. We have confirmed that the unique and accurate time-dependent contact condition can be obtained using this method. Note that there is no displacement error due to the convergent threshold. Value of the increment in the y direction is selected by performing calculations when the increment is changed. It was confirmed that the value 0.1 was small enough for our model, because the change in result was sufficiently small even when the increment value was made smaller. The FE code MARC is used in this paper.

B. Results

Fig. 2 shows the deformation of the elastic finger when the planar surface is indented 1 mm into the elastic finger in the

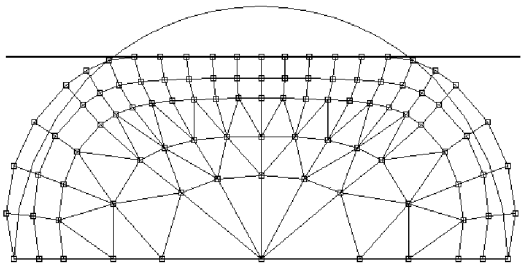

Fig. 2. Deformation of an elastic finger when a plate is indented into the finger by 1 mm.

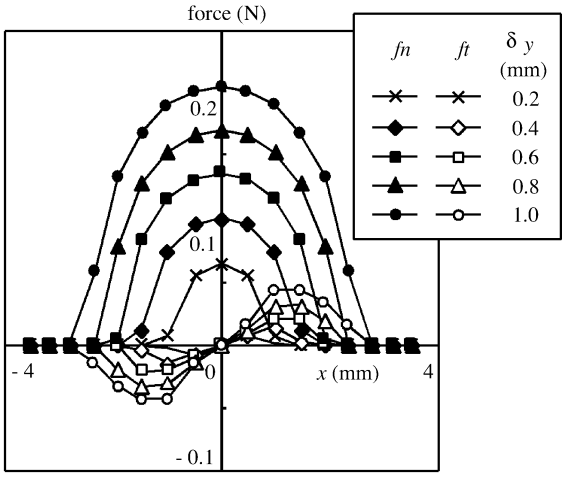

Fig. 3. Reaction force distribution when frictional coefficient is 0.25.

direction normal to the finger surface. Fig. 3 shows a normal and tangential contact force distribution at the surface of the cylindrical finger when the y direction forced displacement of the plate δ_y is from 0.2 to 1 mm. The friction coefficient μ is 0.25.

The normal force distribution is always semicircular because the finger is curved. The tangential reaction force, i.e., the friction force, has a local minimum and a local maximum. The sum of the tangential force is always zero, because no movement of the surface in the x direction is applied. Because the normal force distribution is always semicircular, the limiting friction force, μf_n, is small at the edge of the contact area.

When the indentation is increased, the tangential reaction force or friction force f_t reaches the limiting friction force μf_n near the edges of the contact area. Then these regions slip, and a kinetic friction force is applied. Two slip regions at the edge of the contact area and a stick region at the center are produced when the plate is indented 1 mm into the elastic finger, as shown in Fig. 4. When the indentation is increased, the partial incipient slip regions at both edges of the contact region increase.

Fig. 5 shows the results when the planar surface is indented 1 mm into the elastic finger and the friction coefficient is 0.25. The data is plotted for the normal strain distribution ε_x, ε_y, and shear strain distribution γ_{xy} inside the elastic finger at the nodes shown as circles in Fig. 1. The distribution of the shear strain γ_{xy} changes as a function of the change in the tangential contact force, whereas the distribution of normal strains ε_x and ε_y do not change noticeably. The change in the stick/slip condition

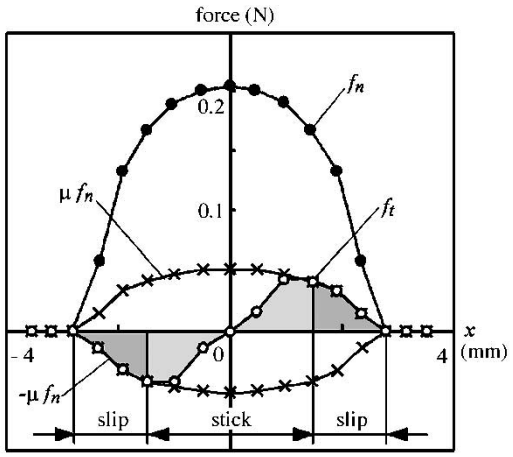

Fig. 4. Reaction force distribution when the plate is indented into the elastic finger by 1 mm ($\mu = 0.25$).

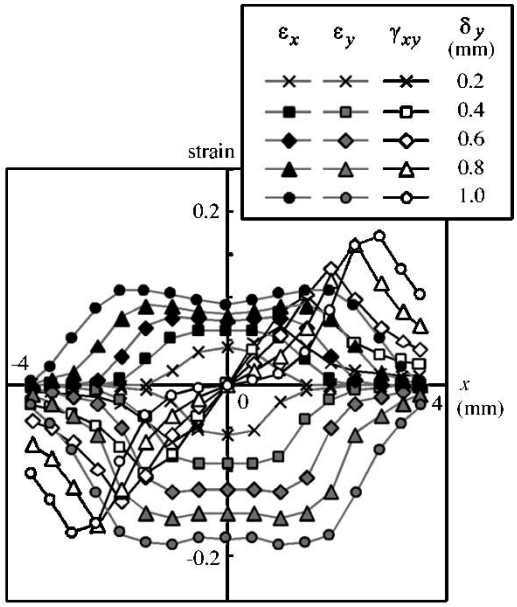

Fig. 5. Strain distribution when the plate is indented into the elastic finger by $\delta_y(\mu = 0.25)$.

appears to affect the change in the shear strain. This is the same phenomena as was shown in our previous study [7]. This implies that the shear strain must include information relating to the stick/slip condition and the value of the friction coefficient. Therefore, we conducted the FE analysis for different friction coefficients μ.

Fig. 6 shows the normal and tangential reaction force distribution when the surface is indented 1 mm into the elastic finger. The friction coefficients μ used in the calculation are 0.06, 0.125, 0.25, 0.5, and 1.0. The normal reaction force f_n does not differ greatly. On the other hand, the tangential reaction force, f_t, differs in relation to the friction coefficient. This is due to the fact that the limiting friction force μf_n, which is shown in Fig. 4, differs when the friction coefficient differs. When the friction coefficient μ is large, the value of the tangential force is large, whereas the area of the slip region at the edge of the contact area is small. This is due to the following phenomena. The nodes at the edge of the contact area are constrained in the

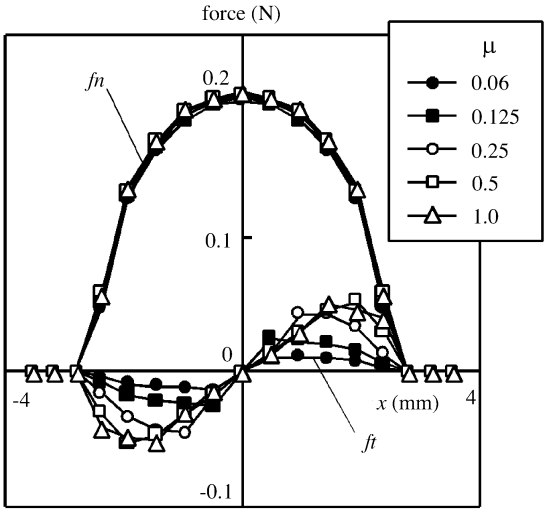

Fig. 6. Reaction force distribution when frictional coefficient is changed.

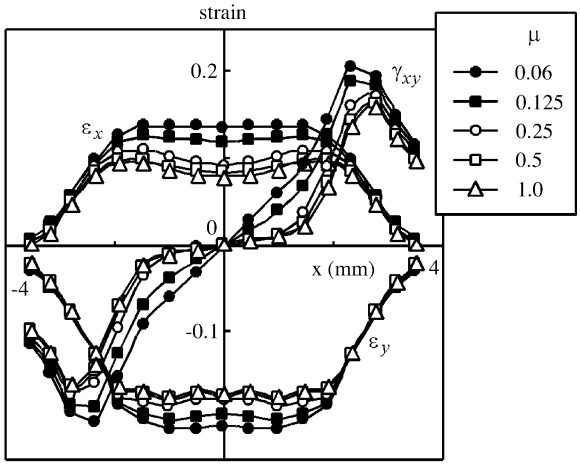

Fig. 7. Strain distribution when the plate is indented into the elastic finger by 1 mm for various frictional coefficients.

x direction because a node sticks when the friction coefficient is large enough to satisfy (3). On the other hand, when the friction coefficient is small, the constraint on the nodes is released, because the nodes slip and (4) is satisfied.

Fig. 7 shows the results when a planar surface is indented 1 mm into the elastic finger and the friction coefficient is changed from 0.06 to 1.0. The data is plotted for the normal strain distribution ε_x, ε_y, and the shear strain distribution γ_{xy} inside the elastic finger at the nodes shown as circles in Fig. 1. The distribution of the normal strains ε_x and ε_y, and the shear strain γ_{xy}, change as a function of the friction coefficient. Hence, Shinoda [12] used the change in tangential stress/strain at $x = 0$ to estimate the friction coefficient. However, the changes in tangential strain ε_x are not large, because the slip area at the edge of the contact area does not much effect the changes in tangential stress/strain at $x = 0$. Therefore, the shear stress/strain near the slip area should be used to estimate the friction coefficient, rather than the tangential stress/strain.

Since the kinetic friction coefficient is usually smaller than the static friction coefficient, we conducted an FE analysis for ratios between the kinetic and static friction coefficients of 0.7, 0.5, and 0.1. Shear strain distribution, when the static friction coefficient is 0.25 and the condition of calculation is the same as that above, is shown in Fig. 8. The shear strain does not vary greatly when the ratio is over 0.5, because change in kinetic friction force of the slip area at the edge of the contact area has little effect. The same characteristics are observed even when the calculation is performed for different static friction coefficients. Hence, we can estimate the static friction coefficient using the proposed method when the ratio between the kinetic/static friction coefficients is larger than 0.5, which is a realistic value for the usual contact surface; whereas the value 0.1 is not realistic.

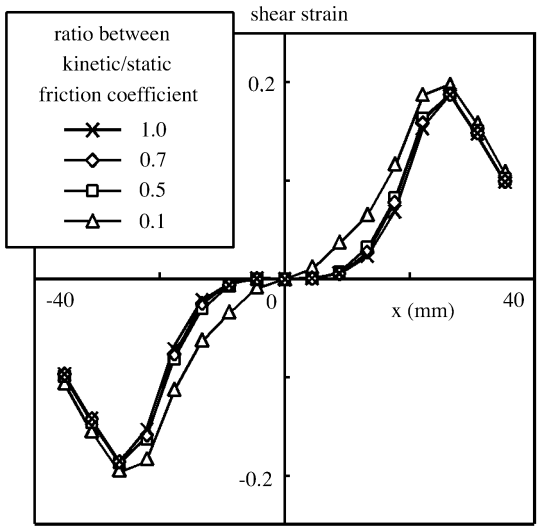

Fig. 8. Shear strain distribution when the ratio between kinetic and static friction coefficients is changed (indentation = 1 mm, static frictional coefficient = 0.25).

Hereafter, the static friction coefficient is referred to as the friction coefficient.

III. FE Analysis for Realistic Design

A. Model

Recently, several kinds of sensors for measuring the shear strain have been proposed [7], [12], [13], and these sensors can be used in obtaining shear strain to estimate the friction coefficient. The simplest technique to detect the shear strain is by measuring the tensile strain using an inclined strain gauge incorporated inside an elastic body. Therefore, we design a finger-shaped sensor made of silicone rubber, into which strain gauges are incorporated.

The half-cylindrical model used in the previous section does not have an optimum geometry with maximized sensitivity for estimating the friction coefficient, particularly when the friction coefficient is large. We, therefore, design in detail the geometry of the sensor used to estimate the friction coefficient up to a large value by calculating the contact condition between the finger-shaped sensor and a planar object. The effects of location and the placement angle of the strain gauge are also calculated in order to determine the location and angle, which provide the maximum sensitivity when estimating the friction coefficient.

In addition to the half-cylindrical model, we also performed calculation using a half cylinder with sections removed from the

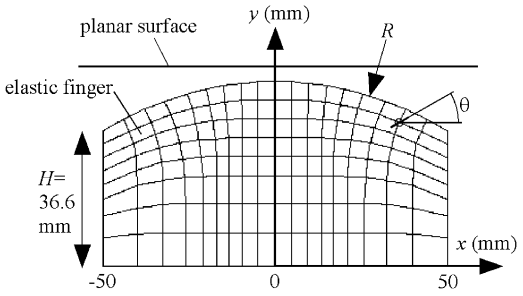

Fig. 9. FE model of the cross-section of the newly designed elastic finger.

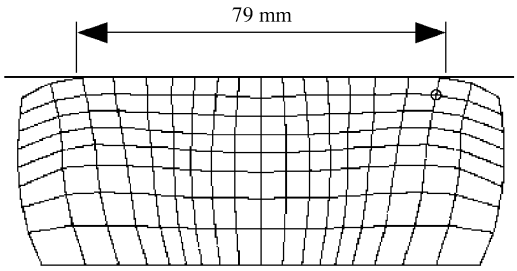

Fig. 10. Deformation of the newly designed elastic finger when a plate is indented into the finger by 10 mm.

corners (see Fig. 9). The radius of the cylinder R and the height of the area removed H are set as variables in the calculation. The indentation depth is fixed at 10 mm. This value is decided so as to verify the method by an experiment without difficulty, and can be changed when the size and geometry of the sensor is changed due to demands of the design. In addition, plane strain elements are used, and nonlinearity due to large deformation is neglected. Nodes at $y = 0$ are fixed.

B. Results

FE analysis for different geometries revealed that a cylinder having a radius of 100 mm and an edge height of 36.6 mm, as shown in Fig. 9, was the most sensitive to changes in the friction coefficient throughout a large range at an indentation depth of 10 mm. Fig. 10 shows the deformation of the elastic finger when a planar surface is indented 10 mm. The contact width is approximately 79 mm. Fig. 11 shows the variation of shear strain with the friction coefficient. When compared to Fig. 7, Fig. 11 reveals a larger change in shear strain for different friction coefficients. In particular, shear strain changes, even when the friction coefficient is large at the node $x = 36$ mm, which circles indicate in Figs. 9 and 10. This is because the position $x = 36$ mm is near the edge of the contact area. The area near the edge of contact slips easily because both sides of the finger have been removed. Fig. 12 shows the change in normal strain at the node at $x = 36$ mm when the angle of strain gauge θ (see Fig. 9) is changed. The normal strain along the inclined axis acts similar to shear strain. The strain is large when the angle is large; however, when the angle is 30°, the change in strain is rather linear over the entire range of friction coefficients. Thus, we decided to estimate the change in friction coefficient via measuring the normal strain by using a strain gauge located at $x = 36$ mm, which is set at an angle of 30°.

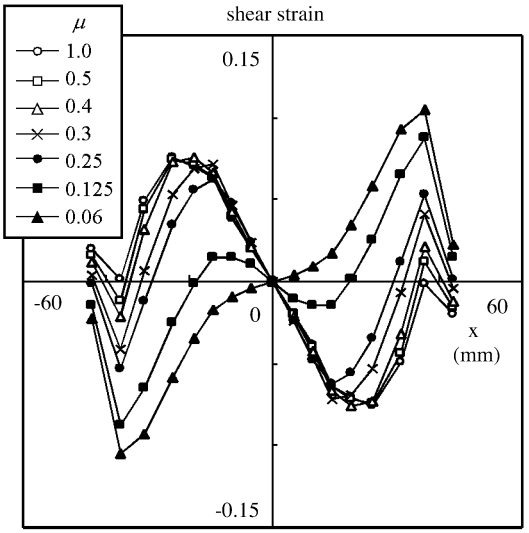

Fig. 11. Shear strain distribution of the newly designed finger-shaped sensor.

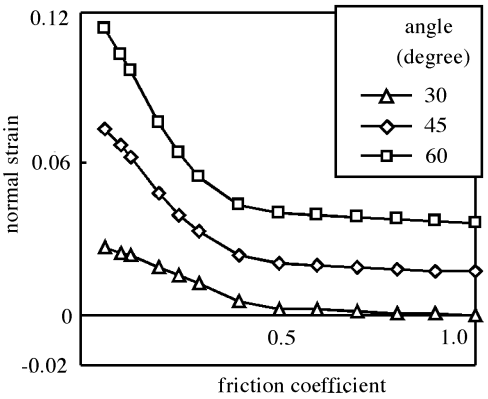

Fig. 12. Calculated normal strain of strain gauges when the angle of the strain gauge at $x = 36$ mm is changed.

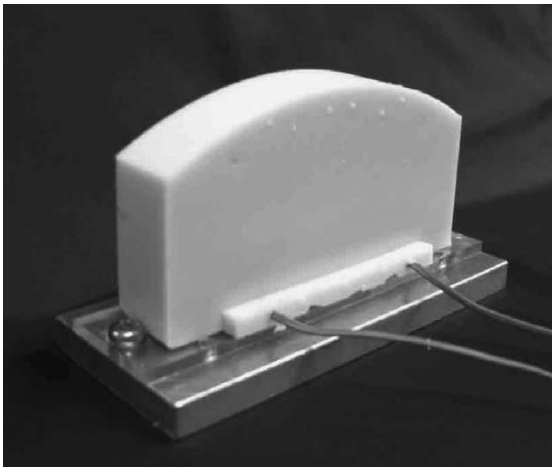

Fig. 13. Newly designed elastic finger-shaped sensor.

IV. Development and Measurement of the Sensor

The newly designed finger-shaped sensor is constructed using silicone rubber and a strain gauge. Fig. 13 shows the newly developed sensor. The strain gauge is embedded directly inside the

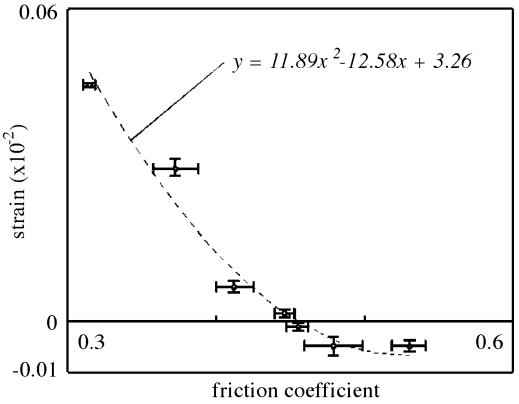

Fig. 14. Relationship between friction coefficient and measured strain.

silicone rubber at the location shown in Fig. 9. The width of the sensor is 20 mm.

Seven objects having planar surfaces are prepared. The friction coefficients between these surfaces and a silicone rubber having a flat surface are measured ten times in advance. Next, the strain of the finger-shaped sensor is measured when the sensor is indented 10 mm into the object. Ten measurements are performed for each object. The relationship between the measured friction coefficient and the strain is shown in Fig. 14. The line in Fig. 14 indicates a second-order equation for approximating the seven points. Vertical and horizontal bars around the measured points represent standard deviation. The figure shows the difference in friction coefficient for the seven objects. In addition, the strain is small when the friction coefficient is large, which matches the calculated result shown in Fig. 12.

The largest standard deviation of strain is 1.5×10^{-4}. The error of the friction coefficient using the second-order equation and standard deviation is 0.1. The minimum friction coefficient was derived from the equation when $\mu = 0.5$. Hence, the friction coefficient can be measured with an accuracy of 0.1–0.5 using the newly developed finger-shaped sensor. Thus, the proposed method is confirmed using actual equipment. Repeatability of the sensor is not completely satisfactory for distinguishing the friction coefficient around 0.5. This is because the slip area at the edge of the contact area does not largely differ when the friction coefficient is large. However, it is not necessary for a robot finger to distinguish the friction coefficient at this range, because large slip area followed by slip down of the object does not easily occur when the friction coefficient at the surface of the object is large. This experiment is performed by increasing the indentation slowly to avoid the effect of viscosity of the sensor. Analysis on the effect of viscosity is also a topic for the future study.

V. Conclusion

We have proposed a method for estimating the friction coefficient between an object and a cylindrical elastic finger-shaped sensor by pressing the elastic finger against the planar surface. The contact problem has been solved between the half-cylindrical finger and planar surface with different friction coefficients when the surface is indented into the finger. The shear strain is useful for estimating the friction coefficient between the two bodies. An elastic sensor having a curved surface is designed and constructed in order to verify the correctness of the FE simulation and to demonstrate that the friction coefficient can be estimated.

Miniaturization of the sensor and applications to the nonflat, elastic, and three-dimensional objects are topics for future study. The proposed method is based on the estimation of the partial-slip phenomena, which always occur, even when the parameters shown above are changed. Hence, the method is fundamentally applicable, even when the size, indentation depth, geometry, and elasticity of the object are changed according to the condition of applications. In such cases, the geometry of the sensor should be modified by FE contact analysis, similar to this paper.

References

[1] R. W. Patterson *et al.*, "The induced vibration touch sensor—A new dynamic touch sensing concept," *Robotica*, vol. 4, pp. 27–31, 1986.
[2] D. Dornfeld *et al.*, "Slip detection using acoustic emission signal analysis," in *Proc. IEEE Int. Conf. Robotics and Automation*, 1987, pp. 1868–1875.
[3] R. D. Howe and M. R. Cutkosky, "Sensing skin acceleration for slip and texture perception," in *Proc. IEEE Int. Conf. Robotics and Automation*, 1989, pp. 145–160.
[4] P. Dario *et al.*, "Planning and expecting tactile exploratory procedures," in *Proc. IEEE/RSJ Int. Conf. Intelligent Robots and Systems*, 1992, pp. 1896–1903.
[5] M. Tremblay and M. R. Cutkosky, "Estimating friction using incipient slip sensing during a manipulation task," in *Proc. IEEE Int. Conf. Robotics and Automation*, 1993, pp. 429–434.
[6] G. Canepa and D. D. Rossi *et al.*, "Detection of incipient object slippage by skin-like sensing and neural network processing," *IEEE Trans. Syst., Man, Cybern. B*, vol. 28, pp. 348–356, Mar. 1998.
[7] T. Maeno *et al.*, "Analysis and design of a tactile sensor detecting strain distribution inside an elastic finger," in *Proc. IEEE/RSJ Int. Conf. Intelligent Robots and Systems*, 1998, pp. 1658–1663.
[8] S. Johansson and G. Westling, "Signals in tactile afferents from the fingers eliciting adaptive motor responses during the precision grip," *Exp. Brain Res.*, vol. 66, pp. 141–154, 1988.
[9] A. Bicchi, "Intrinsic contact sensing for soft fingers," in *Proc. IEEE Int. Conf. Robotics and Automation*, vol. 2, 1990, pp. 968–973.
[10] A. Bicchi, J. K. Salisbury, and D. L. Brock, "Experimental evaluation of friction data with an articulated hand and intrinsic contact sensors," in *Experimental Robotics—II*, R. Chatila and G. Hirzinger, Eds. New York: Springer-Verlag, 1994, vol. 190, Lecture Notes in Control and Information Sciences, pp. 153–167.
[11] Y. Yamada *et al.*, "Active sensing of static friction coefficient," in *Proc. ICAR*, 1993, pp. 185–190.
[12] H. Shinoda, "Instantaneous evaluation of friction based on ARTC tactile sensor," in *Proc. IEEE Int. Conf. Robotics and Automation*, 2000, pp. 2173–2178.
[13] H. Shinoda, K. Matsumoto, and S. Ando, "Acoustic resonant tensor cell for tactile sensing," in *Proc. IEEE Int. Conf. Robotics and Automation*, 1997, pp. 3087–3092.

Takashi Maeno (M'03) was born in Yamaguchi, Japan, on January 19, 1962. He received the B.S., M.S., and Ph.D. degrees in mechanical engineering from the Tokyo Institute of Technology, Tokyo, Japan, in 1984, 1986, and 1993, respectively.

From 1986 to 1995, he was with Canon, Inc., in Tokyo, Japan. Since 1995, he has been with the Department of Mechanical Engineering, Keio University, Yokohama, Japan, where he is currently an Associate Professor. He was a Visiting Industrial Fellow at the University of California, Berkeley, from 1990 to 1992, and a Visiting Scholar at Harvard University, Cambridge, MA, in 2001. His current research interest is in sensors, actuators, and robots.

Tomoyuki Kawamura was born in Sendai, Japan, on May 14, 1977. He received the B.S. and M.S. degrees in mechanical engineering from Keio University, Yokohama, Japan, in 2000 and 2002, respectively.

He is currently with Hitachi Ltd., Yokohama, Japan.

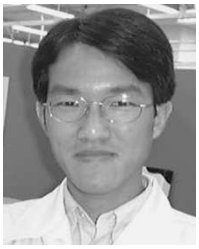

Sen-Chieh Cheng was born in Chiai, Taiwan, on March 30, 1970. He received the B.S. degree in mechanical engineering and M.S. degree in biomedical engineering from Keio University, Yokohama, Japan, in 1998 and 2000, respectively.

He is currently with Shinkawa Ltd., Tokyo, Japan.